An interaction integral method for 2D elastodynamic crack problems

Zhiyong Wang[1], Li Ma[1,*], Linzhi Wu[1], Hongjun Yu[2]

[1] Center for Composite Materials and Structures, Harbin Institute of Technology, Harbin 150001, PR China
[2] Institute of Applied Mathematics, Harbin Institute of Technology, Harbin 150001, PR China
* Corresponding author: mali@hit.edu.cn

Abstract In this paper, a domain formed interaction integral is derived for the evaluation of dynamic stress intensity factors (DSIFs) for arbitrary 2D cracks in non-homogeneous materials. The interaction integral is formulated by superimposing the actual and auxiliary fields on the path independent *J*-integral. By selecting the appropriate auxiliary fields, the derived interaction integral does not involve any derivatives of material properties compared to the available expressions in the literature. Moreover, it can be proved that the integrand is valid even when the integral domain contains material interfaces. Therefore, the integrand is simpler in form and it can be applied in more general situations. The numerical implementation of the new expression of interaction integral is then combined with the extended finite element method (XFEM) without tip enriched functions and a benchmark and test problem is presented. Finally, a non-homogeneous cracked body under dynamic loading is employed to investigate dynamic fracture behavior such as the variation of DSIFs for different material properties.

Keywords Interaction integral, dynamic stress intensity factors, XFEM without tip enriched functions

1. Introduction

Dynamic stress intensity factors (DSIFs) are crucial fracture parameters in understanding and predicting dynamic fracture behavior of a cracked body. To evaluate DSIFs for both homogeneous and non-homogeneous materials, numerous methods have been developed. Among these methods, the numerical techniques may be the most convenient and reliable ones to determine the fracture parameters for more complicated cases, as discussed below.

For homogeneous materials, Kishimoto et al. proposed a modified path-independent *J*-integral, which involves the inertial effects to determine DSIFs combined with the finite element method (FEM), and employed a decomposition procedure for mixed-mode problems [1]. Soon after, Nishioka et al. derived another dynamic *J*-integral to determine DSIFs for non-homogeneous materials [2]. However, the derived integrand is not well-suited for the finite element method. Kim et al. derived an equivalent domain form of the *J*-integral by using the divergence theorem and some additional assumptions [3]. As we known, it is difficult to extract mixed-mode DSIFs using *J*-integral. Instead, the interaction integral, which is known to be superior to both the displacement correlation technique (DCT) and *J*-integral, may be a suitable choice. Song et al. presented a domain formed interaction integral, namely *M*-integral, to investigate the DSIFs for homogeneous and smoothly non-homogenous materials [4]. In the formulation, the non-equilibrium formed auxiliary fields are employed, which have been discussed by Kim et al [5] and Dolbow et al. [6]. More recently, Réthoré et al. presented an interaction integral based on Lagrangian conservation for the estimation of DSIFs for arbitrary 2D moving cracks [7]. Most of the previous works are concerned with the materials with continuous and differentiable properties. If the above conditions are not met, the applications of the interaction integral method are impeded. Moreover, very few published papers have considered the cases that there are several material interfaces in the interaction integral domain. Actually, such phenomenon generally exists.

In this paper, the derivation of an interaction integral and its associated domain form without any derivatives of material properties is presented. We also present the mathematically rigorous proof that the proposed interaction integral method is still valid even when there are material interfaces in the integral domain. Several test problems and the comments are provided in the last section.

2. Numerical Strategy

The interaction integral utilizes two admissible fields: auxiliary and actual fields. Auxiliary fields are based on known fields such as Williams' solution, while actual fields utilize quantities such as displacements, strains and stresses obtained by means of XFEM without tip enriched functions. The choice of the auxiliary fields is discussed firstly. Then, the derivation of the interaction integral and the introduction of the numerical technique will be provided.

2.1. Interaction Integral

In this work, the asymptotic fields of Williams' solution are employed as the auxiliary fields for dynamic non-homogeneous materials, because the dynamic asymptotic fields of non-homogeneous materials show similar behavior to those of quasi-static homogeneous materials around the crack tip [8]. In addition, the incompatibility formulation, proposed by Dolbow et al. [6], is selected. In this formulation, the auxiliary displacements and stresses are obtained directly from Williams' solution and the auxiliary strains are evaluated from the non-homogeneous constitutive model. The auxiliary displacement is given by Eq. (1)

$$u_i^{aux} = \frac{K_I^{aux}}{2\mu_0}\sqrt{\frac{r}{2\pi}}u_i^I(\theta) + \frac{K_{II}^{aux}}{2\mu_0}\sqrt{\frac{r}{2\pi}}u_i^{II}(\theta) \tag{1}$$

The auxiliary stress is given by Eq. (2)

$$\sigma_{ij}^{aux} = \frac{K_I^{aux}}{\sqrt{2\pi r}}\sigma_{ij}^I(\theta) + \frac{K_{II}^{aux}}{\sqrt{2\pi r}}\sigma_{ij}^{II}(\theta) \tag{2}$$

Finally, the auxiliary strain is obtained from

$$\varepsilon_{ij}^{aux} = S_{ijkl}(x)\sigma_{kl}^{aux} \tag{3}$$

where $S_{ijkl}(x)$ is the compliance tensor of the non-homogeneous material.

Since the material property involved in the auxiliary displacement is the local value at the crack tip, the auxiliary strain fields are not compatible with the auxiliary displacement fields. Next, we will focus on the derivation of the interaction integral. The dynamic *J*-integral for cracked homogeneous linear elastic materials is [9]

$$J = \lim_{\Gamma\to 0}\int_\Gamma \left[(W+L)\delta_{1i} - \sigma_{ij}u_{j,1}\right]n_i d\Gamma \tag{4}$$

Superimposing the actual and auxiliary fields on Eq. (4) and one can obtain the interactional part

$$I = \lim_{\Gamma\to 0}\int_\Gamma \left[\frac{1}{2}(\sigma_{jk}^{aux}\varepsilon_{jk} + \sigma_{jk}\varepsilon_{jk}^{aux})\delta_{1i} + \rho\dot{u}_j\dot{u}_j^{aux} - (\sigma_{ij}^{aux}u_{j,1} + \sigma_{ij}u_{j,1}^{aux})\right]n_i d\Gamma \tag{5}$$

The related definitions of the interaction integral are illustrated in Fig. 1. Here, we call attention to an important assumption, namely, the auxiliary stress and strain fields are assumed to be related through the same elasticity tensor as the actual stress and strain fields

$$\sigma_{ij}\varepsilon_{ij}^{aux} = C_{ijkl}(x)\varepsilon_{kl}\varepsilon_{ij}^{aux} = \varepsilon_{kl}\sigma_{kl}^{aux} \tag{6}$$

Due to the way in which we have defined the auxiliary fields and the material property in-homogeneity, the associated terms do not vanish when we employ the divergence theorem. The contour integral is then converted into an equivalent domain integral which involves the term induced by the interface together

$$\begin{aligned} I = &\int_A \left[\sigma_{ij}(S_{ijkl}^{tip} - S_{ijkl}(x))\sigma_{kl,1}^{aux} + \rho\ddot{u}_j u_{j,1}^{aux} - \rho\dot{u}_{j,1}\dot{u}_j^{aux} - \rho\dot{u}_j\dot{u}_{j,1}^{aux}\right]q dA \\ &- \int_A \left[(\sigma_{jk}^{aux}u_{j,k} + \rho\dot{u}_j\dot{u}_j^{aux})\delta_{1i} - (\sigma_{ij}^{aux}u_{j,1} + \sigma_{ij}u_{j,1}^{aux})\right]q_{,i}dA + I^*_{\text{int}erface} \end{aligned} \tag{7}$$

where q is the weight function varying from unity at the crack tip to zero on Γ_B, and

$$\Gamma_B = \Gamma_{11} + \Gamma_{12} + \Gamma_{13} \tag{8}$$

and S_{ijkl}^{tip} is the compliance tensor at the crack tip. As shown in Fig. 1, there is bi-material interface $\Gamma_{interface}$ in the domain and the interface is assumed to be perfectly bonded. Thus, the whole integral domain is divided by $\Gamma_{interface}$ into two parts, i.e., A_1 and A_2. In addition, $I^*_{interface}$ in Eq. (7) denotes the interface integral and will be discussed below.

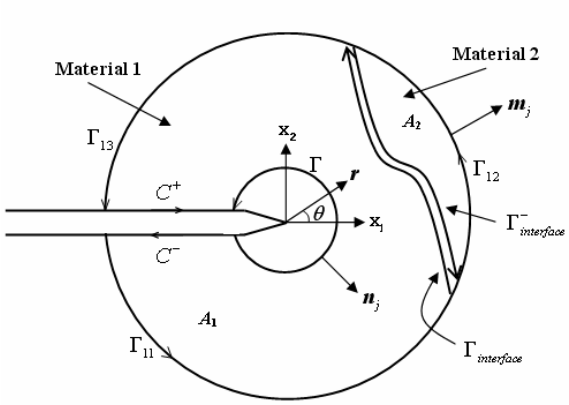

Fig. 1 Interaction integral domain cut by a material interface

The line integral corresponding to the interface can be written as

$$\begin{aligned} I^*_{interface} = \int_{\Gamma_{interface}} \Big[& \sigma_{jk}^{aux}(\varepsilon_{jk}^{(1)} - \varepsilon_{jk}^{(2)})\delta_{1i} - u_{j,1}^{aux}(\sigma_{ij}^{(1)} - \sigma_{ij}^{(2)}) - \sigma_{ij}^{aux}(u_{j,1}^{(1)} - u_{j,1}^{(2)}) \\ & + (\rho^{(1)} - \rho^{(2)})\ddot{u}_j u_{j,1}^{aux}\delta_{1i} \Big] m_i q d\Gamma \end{aligned} \tag{9}$$

To simplify the above equation, we firstly build a curvilinear coordinate system, as shown in Fig. 2.

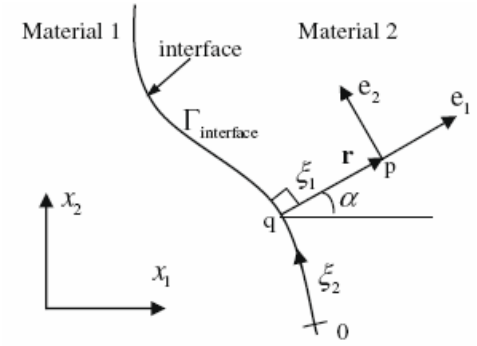

Fig. 2 A curvilinear coordinate system originating from the interface

Then, we have

$$\begin{aligned} \xi_1 &= \sqrt{(x_1 - x_{10})^2 + (x_2 - x_{20})^2} = r \\ \xi_2 &= \int_0^q dl \end{aligned} \tag{10}$$

$$\begin{aligned} \frac{\partial \xi_1}{\partial x_1} &= \cos\alpha = m_1 \\ \frac{\partial \xi_1}{\partial x_2} &= \sin\alpha = m_2 \end{aligned} \tag{11}$$

where (x_1, x_2) and (x_{10}, x_{20}) are the global coordinates of the point *p* and *q*, respectively. (ξ_1, ξ_2) are the curvilinear coordinates of the point *p*. m_1 and m_2 denotes the components of the outward

normal vector $\mathbf{m}$ to $\Gamma_{interface}$ at point q. According to the equilibrium condition on the bi-material interface, the tractions on both sides of the interface should be equal. We have

$$\mathbf{m}\cdot\boldsymbol{\sigma}^{(1)} = \mathbf{m}\cdot\boldsymbol{\sigma}^{(2)} \tag{12}$$

Since the interface is perfectly bonded, the derivatives of actual displacements with respect to the curvilinear coordinate ξ_2 are equal on both sides of the interface, as a result

$$\left(\frac{\partial \mathbf{u}}{\partial \xi_2}\right)^{(1)} = \left(\frac{\partial \mathbf{u}}{\partial \xi_2}\right)^{(2)} \tag{13}$$

According to the above assumptions, it can be found that the first term of the interface integral is equal to the third one, and the second term is zero. If the mass density of the materials on both sides of the interface is equal to each other, we can obtain

$$I^{*}_{interface} = 0 \tag{14}$$

In addition, we assign the values auxiliary velocity fields to zero. The interaction integral (*I*-integral) indicated in Eq. (7) can be simplified as

$$\begin{aligned} I = &\int_A \left[\sigma_{ij}(S^{tip}_{ijkl} - S_{ijkl}(x))\sigma^{aux}_{kl,1} + \rho\ddot{u}_j u^{aux}_{j,1}\right] q dA \\ &- \int_A \left[\sigma^{aux}_{jk} u_{j,k}\delta_{1i} - (\sigma^{aux}_{ij} u_{j,1} + \sigma_{ij} u^{aux}_{j,1})\right] q_{,i} dA \end{aligned} \tag{15}$$

In order to show the advantages of Eq. (15), we will compare it with the traditional *J*-integral and the *M*-integral given by Song et al. [4]. The *J*-integral in the form of the stiffness can be expressed as

$$J = \int_A (\sigma_{ij} u_{i,1} - W\delta_{1j}) q_{,j} dA + \int_A (\rho\ddot{u}_i u_{i,1} - \frac{1}{2} C_{ijkl,1}\varepsilon_{ij}\varepsilon_{kl}) q dA \tag{16}$$

The resulting *M*-integral is

$$\begin{aligned} M = &\int_A \left\{(\sigma^{aux}_{ij} u_{i,1} + \sigma_{ij} u^{aux}_{i,1}) - \sigma^{aux}_{ik}\varepsilon_{ik}\delta_{1j}\right\} q_{,j} dA \\ &+ \int_A \left\{\sigma^{aux}_{ij,j} u_{i,1} + \rho\ddot{u}_i u^{aux}_{i,1} - C_{ijkl,1}\varepsilon^{aux}_{kl}\varepsilon_{ij}\right\} q dA \end{aligned} \tag{17}$$

Through rigorous proof, we can conclude that the *M*-integral is totally equivalent to the *I*-integral. However, the expressions are quite different. It can be found that the derivatives of material properties exist unavoidably in both the above equations. Differently, the *I*-integral in Eq. (15) does not involve any derivatives of material properties. Moreover, in certain conditions, the *I*-integral is still valid even when the integral domain contains material interfaces. Therefore, the applicable range of the present interaction integral is wider than that of the two methods mentioned above for non-homogeneous materials.

2.2. Extended Finite Element Method without Tip Enriched Functions

By enriching the standard approximation with additional functions, the extended finite element method (XFEM) allows for the modeling of arbitrary geometric features independently of the finite element mesh. This advance has provided a convenient computational tool for modeling discontinuities and their evolvements. However, if both the strong discontinuities i.e., cracks and the weak discontinuities i.e., inclusions exist in the domain, especially when the crack tip approaches near the inclusions, it is difficult to obtain the accurate solutions i.e., stress intensity factors (SIFs) using the XFEM technique. In addition, in the XFEM modeling of cracked problems, the corresponding analytical results are pre-requisite. If the analytical solutions are difficult to obtain or are very complex themselves, the application is not convenient. Based on the above reasons, Wang et al. proposed a numerical method, named as extended finite element method without tip enriched functions, for modeling crack growth in particle reinforced composite materials [10]. We employ this numerical method to determine the basic solution of the boundary value

problems. Then, the mixed-mode SIFs can be easily extracted from the Irwins' relation after we get the values of the *I*-integral. The Newmark's method of direct integration schemes is used in dynamic analysis finally.

2.3. Numerical Examples

Young's modulus and mass density vary exponentially, such that $E/\rho \equiv constent$, as given by

$$E = E_0 \exp(\beta_1 x + \beta_2 y) \tag{18}$$

$$\rho = \rho_0 \exp(\beta_1 x + \beta_2 y) \tag{19}$$

where E_0 and ρ_0 are Young's modulus and mass density for initial values. β_1 and β_2 are the non-homogeneity parameters along the *x*- and *y*- directions, respectively. When β_1 and β_2 are equal to zero, the above two equations return to the case of homogeneous materials. A constant Poisson ratio of 0.3 is used during the whole simulation and the plane strain status is assumed. The geometry and the boundary conditions are illustrated in Fig. 3. The data used in the computation are: $L = 20mm$, $D = 40mm$, $2a = 4.8mm$, $E_0 = 199.992GPa$, $\rho_0 = 5000kg/m^3$, $C_d = 7.34mm/\mu s$. The time is normalized with respect to the dilatational wave speed (C_d), and the DSIFs are normalized with respect to

$$K_0 = \sigma_0 \sqrt{\pi a} \tag{20}$$

where the σ_0 is the magnitude of the applied stress and a is half of the total crack length. A time step is $\Delta t = 0.1\mu s$.

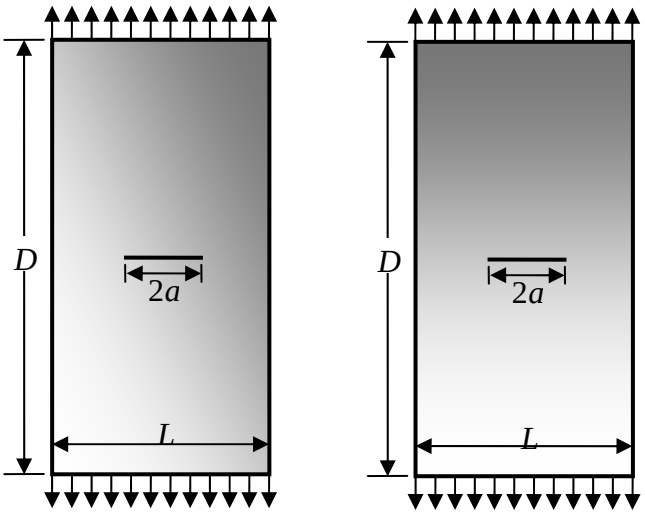

(*a*) (*b*)

Fig. 3 Center cracked tension specimen: (a) non-homogeneous materials (b) exponentially graded materials in the y-direction

In order to employ severe material gradations, relatively high β values are assigned: $\beta_1 = 0.1$ and $\beta_2 = 0.1$. Here, the units corresponding to the material gradation parameters are millimeters. Material properties vary simultaneously along both the *x*- and *y*-directions according to Fig. 3(a). Fig. 4 shows DSIFs at the right crack tip calculated by the present *I*-integral and *M*-integral and the reference ones in the paper written by Song et al. [4]. It can be found that there is an excellent agreement between the present numerical results and the reference ones. It demonstrates that the present method is valid for the fracture problems of such materials.

Next, we consider material properties that vary along the *y*-direction as shown in Fig. 3(b). The material gradation parameter β_1 is set to 0 and β_2 is set as 0, 0.05 and 0.1. Since material properties vary along the *y*-direction, the material properties are the same at both crack tips.

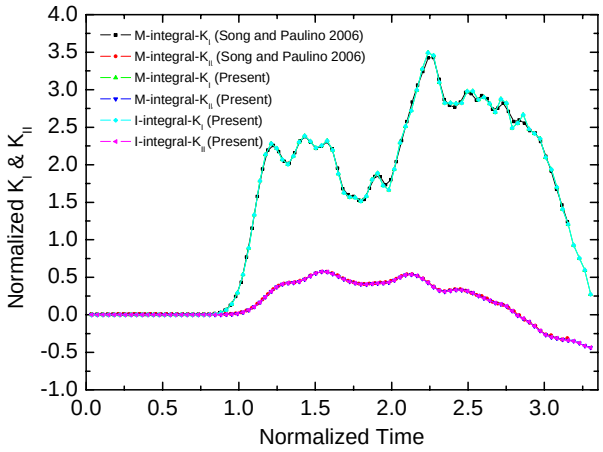

Fig. 4 Normalized DSIFs calculated by different methods

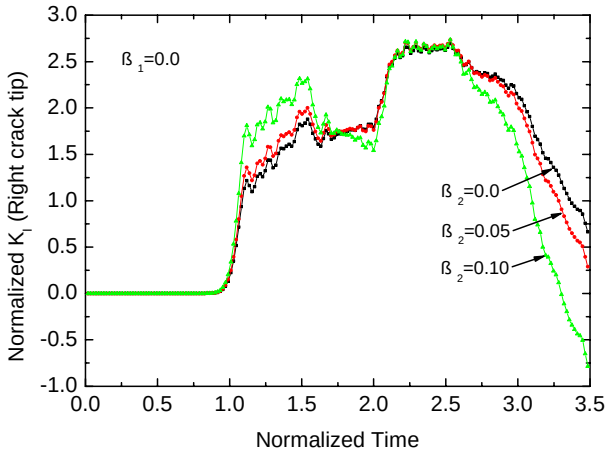

Fig. 5 Normalized mode *I* DSIFs for different material gradations along the *y*-direction

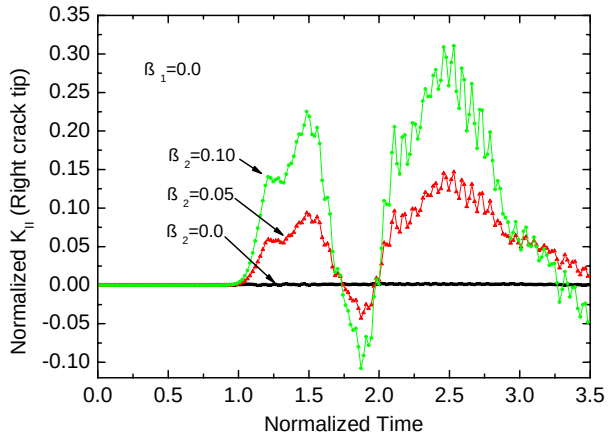

Fig. 6 Normalized mode *II* DSIFs for different material gradations along the *y*-direction

Fig. 5 and Fig. 6 show the mixed-mode DSIFs at the right crack tip. It is obvious that $K_I(t)$ is identical at both crack tips, while the magnitude of $K_{II}(t)$ at the left crack tip is equal in magnitude and opposite in sign to the value at the right crack tip. So we only list the results at the

right crack tip. The initiation time at both crack tips remains the same for all cases of material gradations because of the same definition of material properties. Values of $K_{II}(t)$, induced by material gradients, are more sensitive with increasing β, whereas the maximum magnitude of $K_I(t)$ is relatively insensitive to β. However, the magnitude of $K_{II}(t)$ is relatively small compared to that of $K_I(t)$.

Acknowledgements

This work is sponsored by the National Science Foundation of China under grant Nos. 11222216 and 11202058，the Fundamental Research Funds for the Central Universities under grant No. HIT. NSRIF. 2013082 and China Postdoctoral Science Foundation (20110491071)

References

[1] K. Kishimoto, S. Aoki, M. Sakata, Dynamic stress intensity factors using *J*-integral and finite element method. Eng Fract Mech, 13(1980) 387-394.
[2] T. Nishioka, S.N. Atluri, On the computation of mixed-mode *K*-factors for a dynamically propagating crack using path-independent integrals. Eng Fract Mech, 20(1984) 193-208.
[3] J.H. Kim, G.H. Paulino, The interaction integral for fracture of orthotropic functionally graded materials: evaluation of stress intensity factors. Int J Solids Struct, 40(2003) 3967-4001.
[4] S.H. Song, G.H. Paulino, Dynamic stress intensity factors for homogeneous and smoothly heterogeneous materials using the interaction integral method. Int J Solids Struct, 43(2006) 4830-4866.
[5] J.H. Kim, G.H. Paulino, T-stress, mixed-mode stress intensity factors, and crack initiation angles in functionally graded materials: a unified approach using the interaction integral method. Comput Method Appl M, 192(2003) 1463-1494.
[6] J.E. Dolbow, M. Gosz, On the computation of mixed-mode stress intensity factors in functionally graded materials. Int J Solids Struct, 39 (2002) 2557-2574.
[7] J. Réthoré, A. Gravouil, A. Combescure, An energy-conserving scheme for dynamic crack growth using the extended finite element method. Int J Numer Meth Engng, 63(2005) 631-659.
[8] J.W. Eischen, Fracture of non-homogeneous materials. Int J Fract, 34(1987) 3-22.
[9] B. Moran, F.C. Shih, Crack tip and associated domain integrals from momentum and energy balance. Eng Fract Mech, 27(1987) 615-642.
[10] Z.Y. Wang, L. Ma, L.Z. Wu, H.J. Yu, Numerical simulation of crack growth in brittle matrix of particle reinforced composites using the xfem technique. Acta Mech Solida Sin, 25(2012) 9-21.